AGU PUBLICATIONS

Geophysical Research Letters

RESEARCH LETTER
10.1002/2016GL069106

Key Points:
- Submesoscale motions and turbulent mixing combine to control light-limited phytoplankton growth
- Phytoplankton growth is well described by the critical turbulence hypothesis
- Turbulence induced by submesoscales causes a temporary delay in the onset of the bloom

Supporting Information:
- Supporting Information S1

Correspondence to:
J. R. Taylor,
J.R.Taylor@damtp.cam.ac.uk

Citation:
Taylor, J. R. (2016), Turbulent mixing, restratification, and phytoplankton growth at a submesoscale eddy, *Geophys. Res. Lett.*, *43*, 5784–5792, doi:10.1002/2016GL069106.

Received 13 APR 2016
Accepted 3 MAY 2016
Accepted article online 13 MAY 2016
Published online 11 JUN 2016

Turbulent mixing, restratification, and phytoplankton growth at a submesoscale eddy

J. R. Taylor[1]

[1]Department of Applied Mathematics and Theoretical Physics, University of Cambridge, Cambridge, UK

Abstract High-resolution large-eddy simulations are used to study the influence of submesoscale mixed layer instability and small-scale turbulence on phytoplankton growth in light-limited conditions. Four simulations are considered with small-scale turbulence driven by varying levels of surface cooling. Significant small-scale turbulence is seen even without surface forcing, and the downward mixing of phytoplankton is sufficient to briefly delay the developing bloom. Moderate and strong values of the constant surface heat flux ($Q = -10, -100$ W/m^2) are sufficient to prevent a bloom. In contrast to the critical depth hypothesis, the growth rate for phytoplankton does not appear to be controlled by the mixed layer depth. Instead, a comparison between the turbulent diffusivity above the compensation depth and a critical value predicted by the critical turbulence hypothesis closely matches the timing and magnitude of phytoplankton growth.

1. Introduction

Small free-floating algae known as phytoplankton account for nearly half of the global primary production and form the foundation of the marine food web [*Longhurst et al.*, 1995]. At high latitudes, a strong seasonal cycle in phytoplankton growth and concentration reflects changes in solar insolation, nutrient availability, water temperature, atmospheric forcing, and grazing pressure. A particularly striking feature of the annual cycle in phytoplankton concentration is a rapid growth event known as the spring bloom. Recently, renewed attention has been paid to the physical and biological factors that combine to allow net phytoplankton growth at the onset of the spring bloom (see, e.g., the recent reviews by *Behrenfeld and Boss* [2014], *Sathyendranath et al.* [2015], and the references cited therein). This paper will focus on the physical factors that combine to permit phytoplankton growth and bloom initiation.

Two distinct but related mechanisms have been invoked to explain the influence of physical processes on the onset of phytoplankton blooms. The critical depth hypothesis originating in work by *Gran and Braarud* [1935], *Riley* [1946], and *Sverdrup* [1953] asserts that the depth of turbulent mixing of phytoplankton controls bloom timing. The depth of mixing is often associated with the mixed layer depth, although the active mixing layer does not necessarily coincide with a distinct mixed layer [e.g., *Brainerd and Gregg*, 1995]. If they do not coincide, it might be more appropriate to use the mixing layer depth rather than the mixed layer depth in the critical depth hypothesis [e.g., *Franks*, 2015; *Enriquez and Taylor*, 2015]. Critical turbulence theory, developed by *Huisman et al.* [1999] and *Ebert et al.* [2001], extends the critical depth hypothesis by allowing the strength of turbulent mixing to vary. *Huisman et al.* [1999] predicted that phytoplankton blooms can occur when the turbulent diffusivity drops below a critical threshold, irrespective of mixed layer depth. *Taylor and Ferrari* [2011a] used this framework to link the level of turbulent mixing to convective forcing associated with wintertime surface cooling and proposed that in a homogeneous water column, blooms can develop as soon as the cooling ends—possibly before significant shoaling of the mixed layer and the development of stable density stratification.

When the hydrographic properties of the ocean vary laterally—specifically when there is a significant horizontal density gradient—the level of turbulence in the upper ocean is not only entirely dependent on the level of forcing from the atmosphere and the mixed layer depth but is also influenced by lateral exchange processes. Regions with strong horizontal density gradients, or fronts, are often associated with an along-front "thermal wind" which balances the hydrostatic pressure gradient associated with the change in density. However, the thermal wind equilibrium is unstable to several distinct instabilities. Although their dynamics vary, these instabilities have the net effect of causing the front to slump, thereby increasing the vertical density

gradient—a process known as restratification. This paper will focus on a particular instability termed "mixed layer instability" or MLI, an ageostrophic baroclinic instability that is thought to be important in generating 1–10 km submesoscale eddies in the upper ocean [e.g., *Boccaletti et al.*, 2007; *Fox-Kemper et al.*, 2008; *Thomas et al.*, 2008]. Submesoscales are characterized by relatively large Rossby numbers ($U/(fL) \sim 1$), where U and L are characteristic velocity and length scales and f is the Coriolis parameter [*Thomas et al.*, 2008]. Since the motion is less constrained by the Earth's rotation, submesoscales induce large vertical velocities [*Mahadevan and Tandon*, 2006].

Fox-Kemper et al. [2008] introduced a parameterization for restratification by MLI written in terms of an overturning stream function that acts to flatten tilting isopycnals. Using this parameterization, *Mahadevan et al.* [2010, 2012] defined a restratification ratio comparing the relative importance of eddy-driven restratification and mixing due to wind forcing or convection. Here we will only consider convective forcing. If B_0 is the surface buoyancy flux, the restratification ratio is

$$R_{\mathrm{MLI}} = \frac{B_0 f}{M^4 H^2}, \tag{1}$$

where f is the Coriolis parameter, H is the mixed layer depth, and M is the magnitude of the horizontal buoyancy gradient. Note that *Mahadevan et al.* [2010, 2012] also included a scaling coefficient, $c_e = 0.06$, in the denominator of R_{MLI}. This coefficient is excluded here for simplicity, and all values given below use the form in equation (1).

Restratification by MLI can influence phytoplankton growth in two ways—by decreasing the mixed layer depth and hence the depth of mixing [*Mahadevan et al.*, 2012] and by reducing the intensity of turbulent mixing [*Taylor and Ferrari*, 2011b]. Using two-dimensional numerical simulations, *Taylor and Ferrari* [2011b] found that symmetric and baroclinic instability can restratify the upper ocean and suppress vertical mixing. The resulting phytoplankton blooms were interpreted in terms of the critical turbulence hypothesis. Based on observations from the North Atlantic Bloom 2008 experiment and complementary numerical simulations, *Mahadevan et al.* [2012] observed restratification of the mixed layer before the cessation of wintertime cooling, which the authors attributed to MLI. An increase in the vertically averaged chlorophyll concentration appeared to coincide with the development of stable stratification and preceded the end of winter convection by some 20 days. The authors interpreted the bloom using the critical depth hypothesis with a shoaling of the mixed layer driven by the development of MLI and submesoscale eddies.

The horizontal resolution of the model used in *Mahadevan et al.* [2012] was 1 km. Although their model permitted the development of submesoscale eddies, it was too coarse to resolve turbulent motions in the mixed layer. While the simulations of *Taylor and Ferrari* [2011b] had a much higher resolution (~10 m), they were two-dimensional, preventing them from capturing the rollup of submesoscale eddies and the interaction between small-scale turbulence and mature baroclinic instability. This leaves important open questions: How is small-scale turbulent mixing influenced by the development of submesoscale eddies through MLI and how do phytoplankton respond to submesoscale and fine-scale turbulence in light-limited conditions?

Here high-resolution three-dimensional large-eddy simulations (LESs) are used to examine the competition between turbulent mixing and restratification by MLI and the implications for the onset of the spring bloom. The focus will be on the early stages of development of a submesoscale eddy and phytoplankton bloom, with simulations each running for several days of model time. Small-scale turbulence is forced by applying a uniform surface heat flux. The simulation setup is highly idealized, and relatively small values are chosen for the mixed layer depth and the characteristic size of submesoscale eddies to make the computations more tractable. The simulations are best thought of as numerical experiments rather than an attempt to replicate given ocean conditions. The convective forcing in particular is a useful way to generate small-scale turbulence, although in practice many other factors also contribute to upper ocean turbulence [*Thorpe*, 2005].

A key distinguishing feature of LES is that the largest turbulent motions are explicitly resolved. Therefore, the competition between restratification and mixing by the largest turbulent motions is resolved rather than parameterized. As will be shown below, this distinction has significant implications for the extent and timing of restratification and phytoplankton growth in the simulation. In particular, the net growth of phytoplankton in the LES closely follows the strength of turbulent mixing and does not appear to be set solely by the mixed

Table 1. Simulation Parameters

L_x, L_y, L_z	1000, 1000, 140 (m)
$\Delta x, \Delta y, \Delta z$	2, 2, 1.3–3 (m)
M^2	3×10^{-8} (s^{-2})
f	10^{-4} (s^{-1})
Q	0, −1, −10, −100 (W/m^2)
R_{MLI}	(0, 0.006, 0.06, 0.6)
μ_0, m	1, 0.1 (day^{-1})
h_l	5 (m)

layer depth. This suggests that in addition to shoaling the mixed layer as argued by *Mahadevan et al.* [2012], submesoscales can influence the timing of the spring bloom by modifying the rate of turbulent mixing, consistent with the critical turbulence hypothesis.

2. Simulation Setup

A series of simulations of convectively forced MLI are used to test the competition between turbulent mixing and submesoscale eddy-driven restratification. Although the simulations are highly idealized, they capture important physical processes that influence phytoplankton growth, specifically MLI and convective turbulence. The domain size is 1 km in each horizontal direction and 120 m in the vertical. This domain is resolved with 512 grid points in each horizontal direction and 64 grid points in the vertical. The grid is stretched in the vertical with higher resolution at the upper surface, with a grid spacing ranging from 1.3 to 2.9 m with the highest resolution at the surface. Further details of the numerical method are given in the supporting information.

Periodic boundary conditions are applied in both horizontal directions, and a background buoyancy gradient, $M^2 \equiv |\nabla b|$, is added to the governing equations to represent the influence of a large-scale density gradient. Here we match the background buoyancy gradient in *Mahadevan et al.* [2012] with the choice of $M^2 = 3 \times 10^{-8} s^{-2}$. The buoyancy field is initialized with a weakly stratified "mixed layer" from $-60\ m < z < 0$, overlying a more strongly stratified thermocline. The buoyancy frequency, $N \equiv (\partial b/\partial z)^{1/2}$, is initially uniform in each layer and can be characterized using the "balanced Richardson number" $Ri_B \equiv N^2 f^2 / M^4$, where f is the Coriolis parameter. In this case, the initial conditions prescribe $Ri_B = 1$ in the mixed layer and $Ri_B = 20$ in the thermocline. The weak stratification in the mixed layer ensures that the flow is not unstable to symmetric instability from the start of the simulation. The initial density at the mixed layer base is about 6×10^{-4} kg/m^3 larger than the value directly above at the surface. This density difference is much smaller than the typical thresholds used to define the mixed layer depth, justifying the term "mixed" layer. Based on the initial mixed layer depth ($H = 60$ m) and frontal strength ($M^2 = 3 \times 10^{-8}$ s^{-2}), the fastest growing mode of MLI is expected to have a horizontal scale close to 1 km [*Fox-Kemper et al.*, 2008]. The horizontal domain is therefore large enough to encompass the most unstable mode of MLI. The domain is not large enough to capture mesoscales or the interactions between multiple submesoscale eddies.

The simulations are forced by applying a destabilizing buoyancy flux at $z = 0$, equivalent to cooling the surface. Values of the surface heat flux and R_{MLI} defined in equation (1) are listed in Table 1. *Mahadevan et al.* [2012] found that phytoplankton blooms occur when $R_{MLI} \leq 0.06$. Therefore, the values of R_{MLI} considered here span an order of magnitude above and below the threshold predicted by *Mahadevan et al.* [2012]. Note that while *Mahadevan et al.* [2012] find that $R_{MLI} \simeq 0.06$ for a surface heat flux of $Q \simeq -100$ W/m^2 and the same horizontal buoyancy gradient, our case with $R_{MLI} = 0.06$ corresponds to $Q \simeq -10$ W/m^2. This difference is due to the shallower mixed layer depth used here ($H \simeq 60$ m here, compared with $H \simeq 300$ m in *Mahadevan et al.* [2012]).

The phytoplankton concentration is modeled using the same equation as in *Taylor and Ferrari* [2011a, 2011b]:

$$\frac{\partial P}{\partial t} + \mathbf{u} \cdot \nabla P = \left(\mu_0 e^{z/h_l} - m\right) P + \nabla \cdot \left((\kappa + \kappa_{SGS}) \nabla P\right), \tag{2}$$

where $\mathbf{u}$ is the resolved LES velocity field, μ_0 is the maximum growth rate, h_l is an e-folding depth, m is the mortality (loss) rate, and κ and κ_{SGS} are the constant molecular and subgrid-scale diffusivities, respectively. The parameters in equation (2) match those in *Taylor and Ferrari* [2011a]. Specifically, the maximum growth rate is $\mu_0 = 1$ day^{-1}, the loss rate is $m = 0.1$ day^{-1}, and $h_l = 5$ m. While equation (2) is highly idealized and neglects various factors including nutrient limitation, grazing, self-shading, cell sinking/buoyancy, and motility, it provides a framework to study the influence of turbulence and eddy-driven restratification on phytoplankton

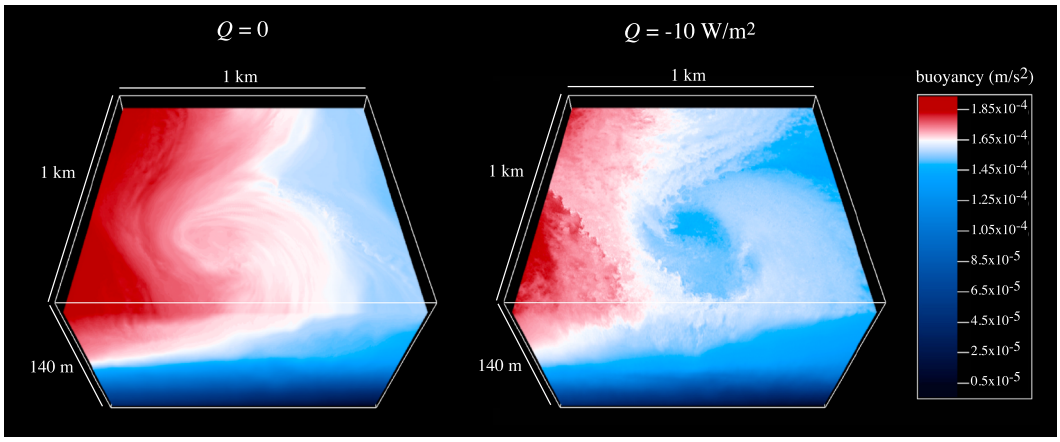

Figure 1. Visualizations of buoyancy at $t = 3.5$ days from simulations with surface heat fluxes of (left) $Q = 0$ and (right) $Q = -10\mathrm{W/m^2}$. An arbitrary constant has been subtracted from the buoyancy such that the minimum value is zero. The upper slice shows the buoyancy at a depth of 10 m.

growth under light-limited conditions. The phytoplankton model is initialized with a constant value $P = P_0$ in the mixed layer, with $P = 0$ below that depth. Since equation (2) is linear in P, the results will be independent of P_0. The simulation parameters are summarized in Table 1.

3. Results

Figure 1 shows visualizations of the buoyancy field at $t = 3$ days for the simulations with no surface cooling ($Q = 0$) and moderate forcing ($Q = -10\ \mathrm{W/m^2}$). In both cases MLI has fully developed by this time and has led to a single coherent submesoscale eddy with a horizontal scale close to the domain size $L \simeq 1$ km, consistent with the most unstable mode associated with MLI. Unlike some previous studies [e.g., *Mahadevan and Tandon*, 2006; *Mahadevan et al.*, 2012; *Fox-Kemper et al.*, 2008; *Capet et al.*, 2008], the resolution used here is sufficient to capture the largest three-dimensional turbulent overturns. In the case with $Q = 0$, small-scale turbulence is visible along the fronts that form at the edge of the submesoscale eddy which is also reflected in enhanced vertical velocity (see the supporting information). Since this simulation is not forced by wind or convection and the flow is initially stable to Kelvin-Helmholtz and symmetric instabilities, the small-scale turbulence that arises is due to a down-scale energy transfer from the submesoscale. As described below, strong vertical motions in this simulation briefly delay the phytoplankton bloom, despite the lack of surface forcing.

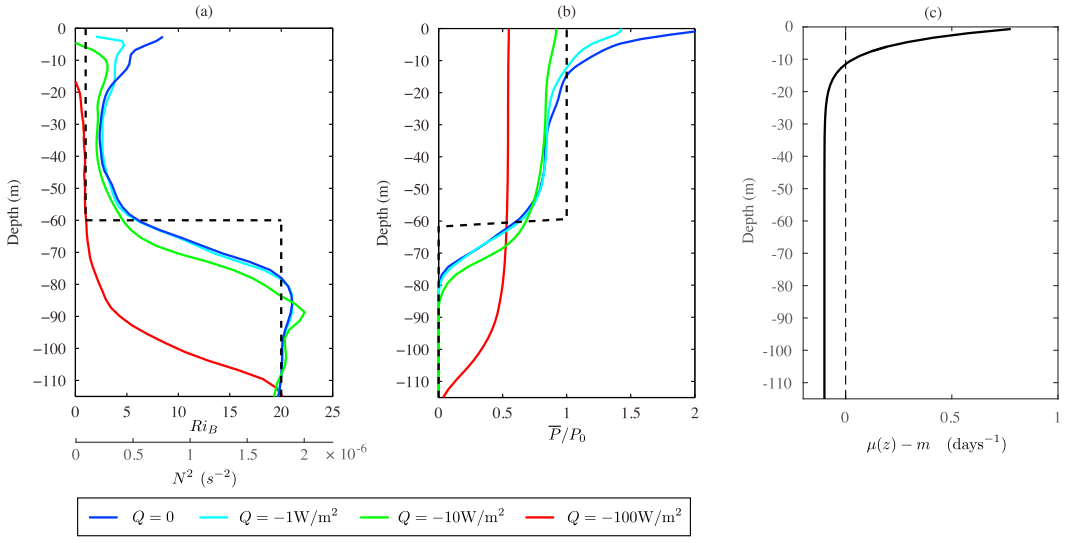

Figure 2. Horizontally averaged profiles of (a) balanced Richardson number, $Ri_B = N^2 f^2 / M^4$, (b) normalized phytoplankton concentration, $\overline{P}/P_0$ at $t = 3$ days, and (c) the net growth rate. Initial profiles are indicated using black dashed lines in Figures 2a and 2b.

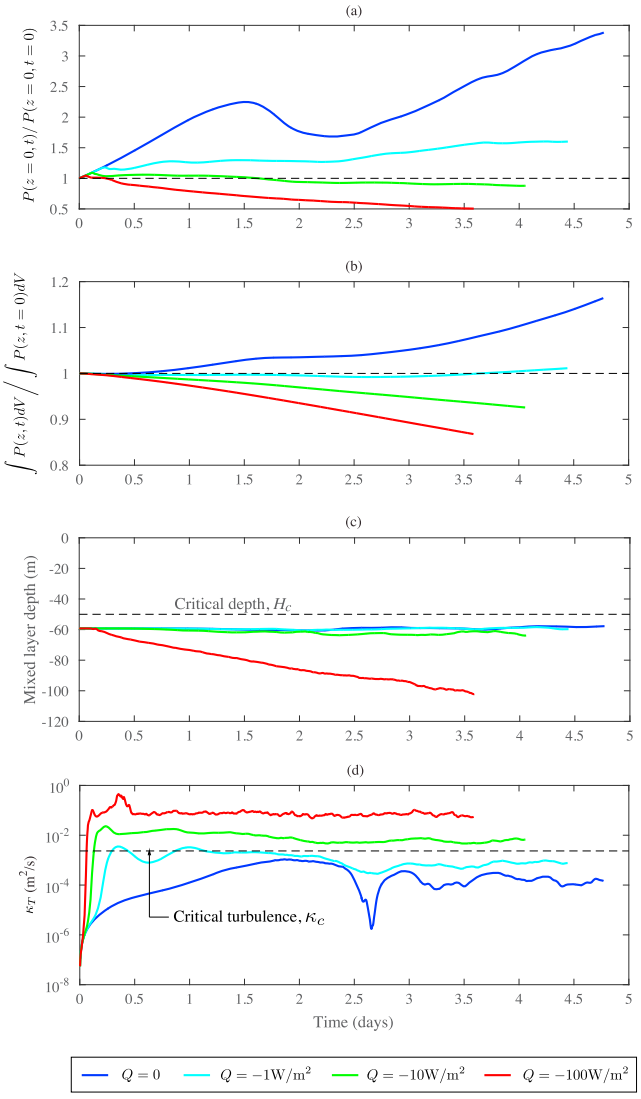

Figure 3. Time series of (a) volume-integrated phytoplankton concentration and (b) diagnosed turbulent diffusivity, κ_T, defined in equation (5). The initial concentration is indicated using a black dashed line in Figures 3a and 3b.

Surface cooling provides another source of small-scale turbulence. In the simulation with $Q = -10$ W/m^2, small convective plumes are visible superimposed on a submesoscale eddy (Figure 1, right).

The competition between restratification by MLI and mixing by small-scale turbulence can be assessed by examining the horizontally averaged stratification. In all cases the mean stratification reaches a nearly steady state after about 2 days. Figure 2a shows profiles of the balanced Richardson number, $Ri_B = \overline{N^2} f^2 / M^4$, where $\bar{\cdot}$ denotes an average over both horizontal directions. Note that here the vertical coordinate is defined to be increasing upward such that $z < 0$. For reference, the initial Ri_B profile is indicated with a dashed line. With the exception of a thin surface layer, the stratification increases relative to the initial state when $Q \geq -10$ W/m^2. Significant deepening of the mixed layer is evident in the case with $Q = -100$ W/m^2, although a weak stable stratification persists in the region between $-70\mathrm{m} < z < -20\mathrm{m}$.

Vertical profiles of the horizontal mean phytoplankton concentration are shown in Figure 2b. For reference, the initial phytoplankton profile is shown using a dashed line. Only the case with $Q = -100$ W/m^2 has a uniform mean phytoplankton profile above the critical depth ($H_c = 50$ m). All other cases show varying degrees of surface intensification, reflecting the net growth rate, $\mu(z) - m$, shown in Figure 2c. Significant spatial variability also develops in the phytoplankton concentration, particularly when the surface heat flux is weak. In the case with Q=0, the phytoplankton concentration at t=3 days varies by more than a factor of 5 at $z = -10$ m (see the supporting information).

Time series of the surface phytoplankton concentration (Figure 3a) show very different behavior among the simulations. Without forcing ($Q = 0$, blue line), phytoplankton grow at the surface for the first 1.5 days, and the surface concentration then decreases briefly before resuming its growth. Very weak convective forcing ($Q = -1$ W/m^2, cyan line) is enough to significantly reduce the increase in the surface phytoplankton concentration. In contrast, aside from a brief spin-up period, the surface concentration decreases monotonically when $Q = -10$ and -100 W/m^2. Depth-time plots of the horizontally averaged stratification and phytoplankton concentration can be found in the supporting information.

If phytoplankton remained at the surface and grew unchecked with the net growth rate (0.9 days^{-1}), their concentration would increase by more than a factor of 90 in a 5 day period. In all simulations here, the surface phytoplankton concentration is much less than the maximum possible growth. Since the phytoplankton model (equation (2)) has a constant net growth rate, limitation of the surface phytoplankton growth must occur through downward advection or diffusion.

The time evolution of the integrated phytoplankton biomass can be calculated by integrating equation (2) over the full model domain. Due to the use of periodic boundary conditions in the horizontal directions and a no flux boundary condition at the top boundary, the integrated phytoplankton biomass satisfies a simple equation

$$\frac{\partial}{\partial t}\int_V P\mathrm{d}V = L_x L_y \int_{-L_z}^{0} \left(\mu_0 e^{z/h_l} - m\right)\overline{P}\mathrm{d}z, \tag{3}$$

where L_x, L_y, and L_z are the dimensions of the full computational domain and $\overline{P}$ is the horizontal mean phytoplankton concentration. The growth of integrated biomass depends only on the vertical structure of $\overline{P}$. Time series of the integrated phytoplankton biomass, $\int P\mathrm{d}V$, are shown in Figure 3a. In the cases with $Q = -10$ W/m^2 and $Q = -100$ W/m^2, $\int P\mathrm{d}V$ decreases monotonically. When $Q = -1$ W/m^2, $\int P\mathrm{d}V$ remains nearly constant, while only the case without forcing ($Q = 0$) exhibits strong growth.

It is clear from Figure 2a that the weakly stratified mixed layer deepens in the simulation with the strongest forcing ($Q = -100$ W/m^2). However, it is not clear precisely how to define the time-dependent mixed layer depth, particularly when a stable stratification develops at the surface. *Mahadevan et al.* [2012] defined the mixed layer depth as the location where the potential density is 0.01 kg/m^3 larger than that at the surface. With this definition, the mixed layer base is deeper than 100 m and well below the critical depth in all cases. A much more sensitive threshold of $\Delta\rho = 6 \times 10^{-4}$ kg/m^3 tuned to match the initial density change in the upper 60 m does yield shoaling of the mixed layer when $Q = 0$, -1, and -10 W/m^2, but the mixed layer depth is very similar in these three cases (the mixed layer depth evolution using both definitions is shown in Figure S7 in the supporting information). The ambiguity in the definition of mixed layer depth is one of the inherent difficulties in applying the critical depth hypothesis to periods of restratification, particularly when the degree of restratification varies with depth.

Figure 3c shows a time series for another choice of the mixed layer depth, defined as the shallowest depth where $N^2 < 5 \times 10^{-7}$ s^{-2}. This value was chosen because it captures the transition from the weakly stratified surface layer to the thermocline in all cases, although as noted above, this is not a unique definition. Defined in this way, the mixed layer base remains below the critical depth in all simulations for all times, which is also the case using the definition in *Mahadevan et al.* [2012]. Notably, the mixed layer depth is nearly identical in the cases with $Q = 0$, -1, and -10 W/m^2, while the mixed layer deepens monotonically when $Q = -100$ W/m^2.

Two perhaps unexpected results have emerged thus far. First, in the unforced simulation ($Q = 0$), the surface phytoplankton concentration decreases between about 1.5 and 2.5 days, and growth in integrated phytoplankton biomass virtually stops before the bloom resumes. Second, the mixed layer depth and stratification profiles are very similar in the cases with $Q = 0$, -1, and -10 W/m^2, but the phytoplankton response in these three simulations is fundamentally different with a surface-intensified bloom when $Q = 0$ and decay when $Q = -10$ W/m^2. Both results can be explained by invoking the critical turbulence hypothesis and examining the intensity of turbulent mixing.

Taylor and Ferrari [2011a] used a simple model to interpret bloom onset via the critical turbulence hypothesis by comparing characteristic time scales associated with net phytoplankton growth and mixing in two layers separated by the compensation depth, h_c, where the local growth rate exactly balances the local loss rate. Using this model, they derived an approximation to the critical turbulent diffusivity,

$$\kappa_c \simeq h_c^2 \frac{\mu_{\mathrm{eff}}^2}{m_{\mathrm{eff}}}, \tag{4}$$

where μ_{eff} is a representative growth rate above the compensation depth and m_{eff} is a representative net loss rate below the compensation depth. Note that μ_{eff} and m_{eff} are both constants in this expression. The critical turbulence hypothesis then predicts net phytoplankton growth when the turbulent diffusivity, κ_T, is less than the critical κ_c.

The turbulent diffusivity can be directly diagnosed from the phytoplankton budget in the simulations presented here. However, the turbulent diffusivity varies in space and time, making a comparison with κ_c more difficult. Nevertheless, we can construct a representative turbulent diffusivity to compare with κ_c by averaging

the vertical flux and the vertical gradient of phytoplankton over the three-dimensional volume above the compensation depth, i.e.,

$$\kappa_T \equiv -\frac{\langle wP \rangle}{\langle \partial P/\partial z \rangle}, \tag{5}$$

where angled brackets denote an average over all points above the compensation depth ($z > h_c$). When defined pointwise rather than using a volume average, κ_T is very noisy and can become large in magnitude or negative, particularly where $\partial P/\partial z$ is small. The choice of the compensation depth as the lower bound of the volume window is motivated by the definition of the critical diffusivity in equation (4) which involves the net growth rate above the compensation depth. The average turbulent diffusivity defined in equation (5) is shown as a function of time in Figure 3b. The critical turbulent diffusivity calculated from equation (4) is shown using a dashed line, where μ_{eff} is calculated by averaging $\mu(z) - m$ above the critical depth, and $m_{\text{eff}} = m$.

For the simulations reported here, the rate of change of integrated phytoplankton biomass, $\int P \mathrm{d}V$, closely follows the turbulent diffusivity defined in equation (5) (see Figures 3b and 3d). Generally, when $\kappa_T < \kappa_C$, the phytoplankton biomass increases, and the converse is also true. The magnitude of the growth and decay in phytoplankton biomass also closely corresponds to the magnitude of κ_T. These results are consistent with the critical depth hypothesis. The correspondence between κ_T and phytoplankton growth is remarkable considering that κ_T is calculated only from model data above the compensation depth (here $h_c \simeq 11$ m).

Submesoscale MLI appears to have two competing influences on the vertical flux of phytoplankton. Without forcing, subduction of phytoplankton associated with MLI is sufficient to temporarily decrease the surface phytoplankton concentration and delay the bloom. On the other hand, restratification suppresses vertical mixing and hence the vertical phytoplankton flux. The outcome of this competition can be quantified by comparing profiles of the turbulent diffusivity from the simulations discussed here with the simulations from *Taylor and Ferrari* [2011a] with the same phytoplankton model but without MLI (see Figure S8). When $Q = -1$ and -10 W/m^2, κ_T is reduced by about a factor of 5 in the simulations with MLI, indicating suppression of mixing by restratification. On the other hand, when $Q = -100$ W/m^2, the profiles of κ_T are very similar identical in the upper 25 m, suggesting that mixing by convection is relatively unaffected by MLI in this region.

4. Discussion

High-resolution large-eddy simulations (LESs) have been used to examine the competition between gravitational slumping of a front (restratification) driven by a submesoscale baroclinic instability and vertical mixing associated with convective forcing. The simulations used a relatively small domain (1 km^2) that is nonetheless large enough to resolve the most unstable mode of mixed layer instability (MLI), while resolving the largest turbulent eddies with a horizontal grid spacing close to 2 m. A fixed background horizontal density gradient supplies potential energy to MLI, and a series of simulations was conducted with different levels of surface cooling. A simplified phytoplankton model is used to examine the impact of this competition on phytoplankton growth under light-limited conditions. In three of the simulations, with surface heat fluxes of $Q = 0, -1, -10$ W/m^2, the stable density stratification increased above the critical depth, and yet only the unforced simulation ($Q = 0$) showed a significant bloom. Weak phytoplankton growth was seen in the simulation with $Q = -1$ W/m^2, while the simulations with $Q = -10$ and -100 W/m^2 exhibited continual decline of the integrated phytoplankton concentration.

The results presented here are not consistent with the hypothesis of *Mahadevan et al.* [2012] that submesoscale eddies trigger phytoplankton blooms by shoaling the mixed layer above the critical depth. Rather, the LES results suggest that phytoplankton blooms can be delayed or suppressed by downward mixing of phytoplankton cells even when a stable stratification develops above the critical depth. The close correspondence between phytoplankton growth and decay and the intensity of turbulent mixing diagnosed using a turbulent diffusivity (Figure 3) suggest that the critical turbulence hypothesis can be used to describe the influence of submesoscales on phytoplankton growth.

There are several important differences between the LES model and the model used by *Mahadevan et al.* [2012] which might explain the difference in the results. The LES directly resolves the largest three-dimensional turbulent motions responsible for mixing phytoplankton in the upper ocean. In contrast, the model used by *Mahadevan et al.* [2012] used a grid spacing of 1 km in the horizontal directions and

parameterized the vertical turbulent mixing. In their model, vertical mixing was parameterized as a prescribed function of depth which was explicitly linked to the mixed layer depth. The magnitude of the vertical mixing coefficient depended on the surface wind stress, but not on the local stratification or shear. Therefore, unlike the LES model used here, the model of *Mahadevan et al.* [2012] does not account for changes in turbulent mixing that might result from stratification within the mixed layer.

On the other hand, the LES model is highly idealized and misses important physical and biological processes. Notably, only convective forcing is considered here, but mixing driven by wind and Langmuir turbulence is likely to be a major factor in setting the intensity of mixing in the upper ocean. Indeed, *Mahadevan et al.* [2012] reported that the vertical velocities observed from a Lagrangian float during the North Atlantic Bloom Experiment were closely correlated with the surface wind stress. The competition between turbulent mixing driven by wind, Langmuir circulation, and restratification by submesoscales has been examined recently [*Hamlington et al.*, 2014; *Smith et al.*, 2016], although the influence of this competition on phytoplankton blooms remains an open question. The phytoplankton model used here also neglects many factors other than light limitation, including grazing pressure which might present another mechanism for triggering the spring phytoplankton bloom [*Behrenfeld*, 2010; *Boss and Behrenfeld*, 2010].

The sensitivity of vertical mixing to the presence of submesoscales presents a major challenge for future observational and modeling work. Turbulent mixing is much more difficult to measure than density stratification, but the results presented here suggest that the former is needed to accurately characterize phytoplankton growth during light-limited conditions. In many ocean modeling applications, it is not feasible to resolve submesoscale dynamics, and the ability to resolve the three-dimensional turbulence responsible for vertical mixing in these cases is well out of reach. A parameterization for MLI was proposed by *Fox-Kemper et al.* [2008] and has already been implemented in several ocean models. The parameterization improves the ability of ocean models to capture the restratification induced by submesoscale eddies, yet does not explicitly modify the turbulent mixing scheme. Further work is needed to examine the direct influence of submesoscale processes on turbulent mixing.

Acknowledgments

J.R.T. was supported by a grant from the Natural Environment Research Council, award NE/J010472/1. The author would like to thank Peter Franks and an anonymous reviewer for very constructive comments, and Raffaele Ferrari, Marina Lévy, Amala Mahadevan, and Adrian Martin for helpful discussions.

References

Behrenfeld, M. (2010), Abandoning Sverdrup's critical depth hypothesis on phytoplankton blooms, *Ecology*, *91*(4), 977–989.

Behrenfeld, M. J., and E. S. Boss (2014), Resurrecting the ecological underpinnings of ocean plankton blooms, *Annu. Rev. Mar. Sci.*, *6*, 167–194.

Boccaletti, G., R. Ferrari, and B. Fox-Kemper (2007), Mixed layer instabilities and restratification, *J. Phys. Oceanogr.*, *37*(9), 2228–2250.

Boss, E., and M. Behrenfeld (2010), In situ evaluation of the initiation of the North Atlantic phytoplankton bloom, *Geophys. Res. Lett.*, *37*, L18603, doi:10.1029/2010GL044174.

Brainerd, K., and M. Gregg (1995), Surface mixed and mixing layer depths, *Deep Sea Res., Part I*, *42*(9), 1521–1543.

Capet, X., J. C. McWilliams, M. J. Molemaker, and A. Shchepetkin (2008), Mesoscale to submesoscale transition in the california current system. Part I: Flow structure, eddy flux, and observational tests, *J. Phys. Ocean.*, *38*(1), 29–43.

Ebert, U., M. Arrayas, N. Temme, B. Sommeijer, and J. Huisman (2001), Critical conditions for phytoplankton blooms, *Bull. Math. Biol.*, *63*, 1095–1124.

Enriquez, R. M., and J. R. Taylor (2015), Numerical simulations of the competition between wind-driven mixing and surface heating in triggering spring phytoplankton blooms, *ICES J. Mar. Sci./J. Conseil*, *72*(6), 1926.

Fox-Kemper, B., R. Ferrari, and R. Hallberg (2008), Parameterization of mixed layer eddies. Part I: Theory and diagnosis, *J. Phys. Oceanogr.*, *38*(6), 1145–1165.

Franks, P. J. (2015), Has Sverdrup's critical depth hypothesis been tested? Mixed layers vs. turbulent layers, *ICES J. Mar. Sci./J. Conseil*, *72*, 1897–1907, doi:10.1093/icesjms/fsu175.

Gran, H., and T. Braarud (1935), A quantitative study on the phytoplankton of the Bay of Fundy and the Gulf of Maine (including observations on hydrography, chemistry and morbidity), *J. Biol. Board Can.*, *1*, 219–467.

Hamlington, P. E., L. P. Van Roekel, B. Fox-Kemper, K. Julien, and G. P. Chini (2014), Langmuir–submesoscale interactions: Descriptive analysis of multiscale frontal spindown simulations, *J. Phys. Oceanogr.*, *44*(9), 2249–2272.

Huisman, J., P. van Oostveen, and F. Weissing (1999), Critical depth and critical turbulence: Two different mechanisms for the development of phytoplankton blooms, *Limnol. Oceanogr.*, *44*(7), 1781–1787.

Longhurst, A., S. Sathyendranath, T. Platt, and C. Caverhill (1995), An estimate of global primary production in the ocean from satellite radiometer data, *J. Plankton Res.*, *17*(6), 1245–1271.

Mahadevan, A., and A. Tandon (2006), An analysis of mechanisms for submesoscale vertical motion at ocean fronts, *Ocean Modell.*, *14*(3), 241–256.

Mahadevan, A., A. Tandon, and R. Ferrari (2010), Rapid changes in mixed layer stratification driven by submesoscale instabilities and winds, *J. Geophys. Res.*, *115*, C03017, doi:10.1029/2008JC005203.

Mahadevan, A., E. D'Asaro, C. Lee, and M. J. Perry (2012), Eddy-driven stratification initiates North Atlantic spring phytoplankton blooms, *Science*, *337*(6090), 54–58.

Riley, G. (1946), Factors controlling phytoplankton populations on Georges Bank, *J. Mar. Res.*, *6*, 54–72.

Rorai, C., P. Mininni, and A. Pouquet (2014), Turbulence comes in bursts in stably stratified flows, *Phys. Rev. E*, *89*(4), 043002.

Sathyendranath, S., R. Ji, and H. I. Browman (2015), Revisiting Sverdrup's critical depth hypothesis, *ICES J. Mar. Sci./J. Conseil*, *72*(6), 1892–1896.

Smith, K. M., P. E. Hamlington, and B. Fox-Kemper (2016), Effects of submesoscale turbulence on ocean tracers, *J. Geophys. Res. Oceans*, *121*(1), 908–933, doi:10.1002/2015JC011089.

Sverdrup, H. (1953), On conditions for the vernal blooming of phytoplankton, *J. Conseil Int. Explor.*, *18*, 287–295.

Taylor, J. R., and R. Ferrari (2011a), Shutdown of turbulent convection as a new criterion for the onset of spring phytoplankton blooms, *Limnol. Oceanogr.*, *56*(6), 2293–2307.

Taylor, J. R., and R. Ferrari (2011b), Ocean fronts trigger high latitude phytoplankton blooms, *Geophys. Res. Lett.*, *38*, L23601, doi:10.1029/2011GL049312.

Thomas, L. N., A. Tandon, and A. Mahadevan (2008), Submesoscale processes and dynamics Ocean Modeling in an Eddying Regime, *Geophys. Monogr. Ser*, *177*, 17–38.

Thorpe, S. (2005), *The Turbulent Ocean*, Cambridge Univ. Press, Cambridge.